Effective dielectric properties of composite materials: The dependence on the particle size distribution

Anna Spanoudaki[1,*] and Rolf Pelster[1,2]
[1]*II. Physikalisches Institut der Universität zu Köln, Zülpicher Strasse 77, 50937 Köln, Germany*
[2]*Institut für Physik und ihre Didaktik, Universität zu Köln, Gronewaldstrasse 2, 50931 Köln, Germany*
(Received 23 December 2000; published 20 July 2001)

We have carried out numerical simulations on the effective transport properties of composites consisting of well separated conductive spherical inclusions in an insulating matrix. The simulations show that the effective permittivity depends markedly on the size distribution of the inclusions. Results are presented in a broad range of filling factors and degrees of polydispersity. For a simple cubic lattice of identical spheres the calculated values agree exactly with the analytical solution. The Maxwell-Garnett model has shown to describe well the case of randomly distributed uniformly sized inclusions independently of the concentration, even at filling factors up to 30%. With increasing degree of polydispersity the permittivity rises towards a limiting value close to the Bruggeman result.

DOI: 10.1103/PhysRevB.64.064205 PACS number(s): 77.84.Lf, 72.80.Tm, 77.22.Ch, 78.20.Ci

I. INTRODUCTION

Its roots going back to the work of Rayleigh[1] and Maxwell,[2] the theory of effective transport properties and especially dielectric properties of composite materials has known considerable development in recent times. In itself, this problem is very interesting, but it also finds direct application in the study of heterogeneous materials such as colloids, porous media, magnetic liquids, ceramics, or artificial dielectrics. Our motivation has been the analysis of dielectric spectra of composites, in order to derive information on the microstructure or on the properties of the dispersed component.[3,4] Although we formulate our results in terms of permittivity, they are valid for all generalized conductivities.

We focus on composites consisting of inclusions embedded in an homogeneous matrix (cermet topology). The effective properties at a given frequency ν are not only a function of the properties of the component materials and of the filling factor, but also depend on shape and spatial distribution of the inclusions. Thus, an analytical solution of the problem can be immensely complicated. An exact analytical solution for an arbitrary spatial configuration of well separated spherical inclusions in a matrix has been presented in Ref. 5. The effective permittivity is expressed in terms of dielectric properties, sizes, and coordinates of the inclusions. In order to calculate the permittivity one still needs the whole detailed information about the microstructure. Thus, the complexity of the problem is not directly reduced. Nonetheless, this analytical solution is an excellent tool to address the problem through exact computer simulations as the ones we present here.

The Maxwell-Garnett[6] model was one of the first approaches to describe the permittivity of random composites. In this mean-field model only an average induced dipole is taken into account for every inclusion. Higher multipole moments are neglected. So, each particle is polarized as if it were in an homogeneous effective field:

$$\varepsilon_{\mathrm{eff}}=\varepsilon_{\mu}\left(1+\frac{1}{A}\frac{fx}{1-fx}\right), \tag{1}$$

where

$$x=\frac{A(\varepsilon_p-\varepsilon_{\mu})}{\varepsilon_{\mu}+A(\varepsilon_p-\varepsilon_{\mu})}. \tag{2}$$

ε_p, ε_{μ} are the dielectric constants of the inclusions and the matrix, respectively, and f is the volume fraction of the particles. The depolarization factor A equals 1/3 in the case of spheres, which is the shape we consider in the following. For conducting inclusions at sufficiently low frequencies $|\varepsilon_p| \gg |\varepsilon_{\mu}|$ holds and thus $x=1$, so that

$$\varepsilon_{\mathrm{eff}}=\varepsilon_{\mu}\frac{1+2f}{1-f}. \tag{3}$$

The Maxwell-Garnett model has been accepted as satisfactory when the exact interparticle interactions are not important, e.g., in the case of dilute dispersions or components of low polarizabilities.

The model that most often shows a good agreement with experimental results (e.g., Refs. 3,4,7,8) is the one derived by Bruggeman[9]

$$\left(\frac{\varepsilon_{\mathrm{eff}}-\varepsilon_p}{\varepsilon_{\mu}-\varepsilon_p}\right)\left(\frac{\varepsilon_{\mu}}{\varepsilon_{\mathrm{eff}}}\right)^{1/3}=1-f, \tag{4}$$

or for conductive particles at low frequencies

$$\varepsilon_{\mathrm{eff}}=\frac{\varepsilon_{\mu}}{(1-f)^3}. \tag{5}$$

This formula, known as the asymmetric Bruggeman or the Hanai-Bruggeman formula, is obtained assuming that the Maxwell-Garnett model is exact at low filling factors and then following an iterative procedure, adding a small fraction of particles at each step. Here, the percolation limit is $f=1$. This model is recognized as valid at least for not too high filling factors and is often used for comparison with experimental data or results of simulations. For other models we refer to Refs. 7,8.

According to the above formulas, the effective permittivity of random cermets depends only on ε_p, ε_μ, and f. However, in Ref. 7 (p. 104) it is noted that measurements on systems with narrow size distributions tend to agree rather with the Maxwell-Garnett than with the Bruggeman model. From the theoretical side, Fu *et al*. have shown that the Maxwell-Garnett formula is within the mean field approximation rigorous to all multipole moments, as long as a spherically symmetric two-particle function describes the spatial distribution of the particles.[10] On the other hand, performing numerical calculations, Barrera *et al*.[11] could show that the Maxwell-Garnett result fails for polydisperse systems. Despite the above experimental and theoretical results there is neither a theoretical model nor a detailed numerical investigation on how ε_{eff} depends on the degree of polydispersity of the inclusions, let us say, on the width of the particle size distribution. The derivation of the abovementioned mean-field approximations does not show in which range they are applicable. Meredith and Tobias[12] have proposed a universal formula for polydisperse systems, but the fact that it does not depend on the degree of polydispersity is a contradiction in terms. The need for a systematic approach is therefore clear. Our numerical investigations, a computer implementation of the exact theoretical solution in Ref. 5, show that the effective permittivity ε_{eff} depends on the particle size distribution in a surprisingly strong way.

II. THE ALGORITHM

In Ref. 5 Fu *et al*. consider a composite material consisting of spherical inclusions of permittivity ε_i in a continuous matrix (cermet topology). The material of total volume V is placed between the plates of an ideal plane capacitor. The plates are separated by a distance d. The authors express the multipole moments developed by the ith particle due to the interactions with other particles and their images, as a function of the particles' dielectric properties ε_i, radii α_i and spatial coordinates:

$$q_{ilm} = \sqrt{\frac{3}{4\pi}} \sum_j \, (G^{-1})^{j10}_{ilm} \beta_{j1} E_0, \tag{6}$$

where

$$\beta_{i1} = \frac{(\varepsilon_i - \varepsilon_\mu)\alpha_i^3}{\varepsilon_i + 2\varepsilon_\mu}, \tag{7}$$

and E_0 is the imposed electric field. The element $G^{jl'm'}_{ilm}(\mathbf{r}_{ij}, \varepsilon_i, \varepsilon_j, l, l', m, m')$ of the two-dimensional configuration matrix G is directly connected with the interaction between the multipole moment (lm) of the ith particle at $\mathbf{r}_i$ and the moment $(l'm')$ of the jth particle at $\mathbf{r}_j$. We denote $\mathbf{r}_{ij} = \mathbf{r}_j - \mathbf{r}_i$. (The exact form of G is given in the Appendix. For details please refer to the original article.) Through the inversion of G all the moments q_{ilm} are mutually dependent. Note especially the coupling of the dipole moments q_{i10} to the higher multipole moments. Fu *et al*. proceed to express the effective permittivity of the composite as follows:

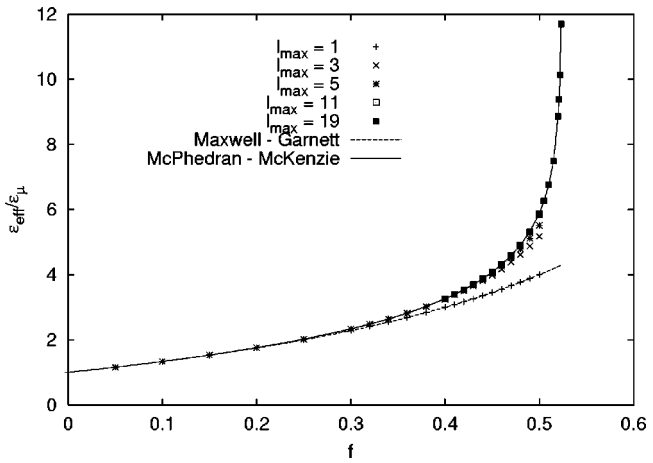

FIG. 1. The ratio of the effective permittivity ε_{eff} over the permittivity of the matrix ε_μ for an sc lattice of conductive spheres. Numerical results taking into account multipole moments up to $l_{\text{max}} = 1,3,5,11,19$ are compared with the Maxwell Garnett model as well as with the exact results by McPhedran and McKenzie.

$$\varepsilon_{\text{eff}} = \varepsilon_\mu \left(1 + \frac{4\pi}{V} \sqrt{\frac{4\pi}{3}} \sum_i \frac{q_{i10}}{E_0} \right)$$

$$= \varepsilon_\mu \left(1 + \frac{4\pi}{V} \sum_{ij} \, (G^{-1})^{j10}_{i10} \beta_{j1} \right). \tag{8}$$

Our simulations are based on this exact solution. A distribution of particles is generated in a cubic shell, the side length of which equals the distance between the electrodes. Periodic boundary conditions are imposed in the directions parallel to the capacitor plates. The configuration matrix elements $G^{jl'm'}_{ilm}$ are computed for each pair of particles and multipole moments. The images and the periodic repetitions of each particle are taken into account (see the Appendix). It is possible to adjust the maximal orders l_{max}, m_{max} of multipole moments considered. More importantly, the algorithm allows simulations of different spatial configurations (ordered, random or nonrandom disordered, isotropic or anisotropic systems) and different size distributions of spherical inclusions. The dielectric properties of matrix and inclusions can be freely chosen, and the composite may even contain inclusions of different permittivities and radii. The results that are presented here were obtained at zero frequency for conductive particles in a matrix of unit dielectric constant. In this case Eq. (7) becomes $\beta_{i1} = \alpha_i^3$. (For $\varepsilon_\mu \neq 1$ the results for the effective permittivity can simply be scaled by a factor of ε_μ [see Eq. (8)].) A detailed report for other cases is to follow.

III. THE SC LATTICE

In order to check the correct implementation of the algorithm as well as the accuracy of our calculations we first treat a simple cubic lattice of identical spheres. This problem has been solved exactly in Refs. 13,14 while accurate measurements are presented in Refs. 15,16. The results are presented in Fig. 1. The diagram shows the effective permittivity of the system as a function of the filling factor. The values pre-

sented have been tested for convergence and are accurate up to the fifth decimal point. There are different sets of points corresponding to calculations for different odd values of the highest multipole $l_{\max}$ taken into account [see Eq. (6)]. Due to the symmetry of the cubic lattice, the multipole moments with even l do not contribute to the polarization. The results are compared with exact values taken from Ref. 14. There is absolute agreement between the analytical formula and our results. This remains true up to the highest filling factor of $f_c=\pi/6\approx 0.5236$, where the spheres touch and the permittivity diverges (percolation limit). In Ref. 14 there are also calculations presented for multipolar moments with $m\neq 0$. The authors point out that their contribution is very small and attribute it to the arithmetical error rather than to a real effect. Our calculations confirm this, giving zero contribution up to the fifth decimal point. Note also that calculations with $l_{\max}=1$, i.e., taking only the interactions of the dipolar moments into account, coincide for all filling factors with the Maxwell-Garnett predictions.

IV. RANDOM DISTRIBUTION

We generated distributions of particles (typically 5000) which were positioned randomly in space filling a cubic volume. The particle size distributions were log normal in volume v with varying width parameter σ (the standard deviation of the correspondent normal distribution):

$$f(v)=\frac{1}{\sqrt{2\pi}\sigma v}e^{-\ln^2(v/v_0)/2\sigma^2}. \tag{9}$$

The median of the volume distribution v_0 can be chosen arbitrarily since the dielectric properties do not change when the sample is scaled in size. Note that Eq. (9) is equivalent to a log-normal distribution of radii with a parameter $\sigma_r=\sigma/3$. Choosing a good algorithm to form the size distribution is of vital importance, since the computing capacity is restricted. Simply using a random numbers generator to pick volumes from a log-normal distribution gives a very poor approximation of the continuous distribution: even at particle populations as high as $N=5000$ this results to strong fluctuations of the particle size distribution density. Of course, for such a configuration the simulation gives a value for ε_{eff} which is physically meaningful, but differs from the value corresponding to a smooth log-normal distribution. Increasing N one should attain an always better approximation but this seems to happen at N too high for our computing capacity. We found that a satisfactory solution to this problem is to use a step function as the one presented in Fig. 2. The v axis is divided in elements dv. Then $[Nf(v_m)]$ particles are homogeneously distributed in the region $(v_m-dv/2,v_m+dv/2]$. For narrow distributions the elements dv may be equal, while for broader distributions (above $\sigma=1.5$) it is recommended to increase dv with increasing v_m. Random coordinates were attributed to each particle, starting from the biggest. In case of overlap with an already positioned particle, new coordinates were chosen. As a consequence, there is no electric contact between neighboring particles. The algorithms for the random distributions, as well as many of the routines used in the main program were modifications of routines found in Ref. 17. Simulations on monodisperse systems were also carried out, using the same positioning algorithm. This algorithm fills the space in a uniform manner with spheres, so that in the case of equally sized inclusions, above a filling factor of 0.3 it is not any more possible to add further particles without overlap. For higher filling factors a different algorithm has to be implemented, that would allow even a random close packed distribution. Of course, there is no such restriction for polydisperse systems, where there is always room for the smallest spheres added towards the end of the procedure.

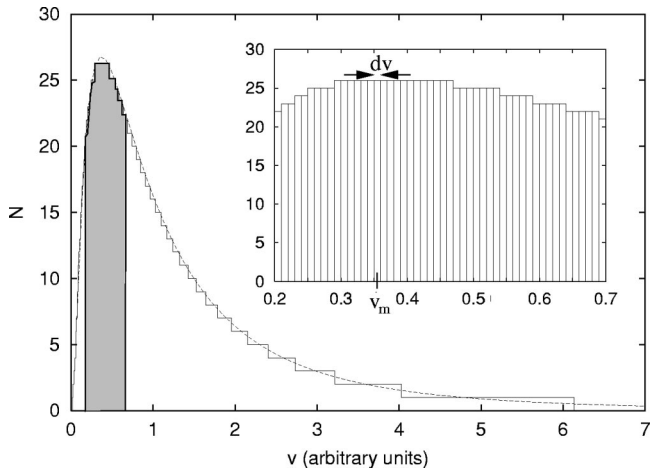

FIG. 2. A volume distribution with $\sigma=1$ and $N=3998$ as it was used for a calculation. The dashed line is the theoretical log-normal distribution. The inset focuses on the shaded part of the graph. In the range $(v_m-dv/2,v_m+dv/2]$ 26 particles are distributed homogeneously.

We have conducted extended simulations involving higher multipole moments, which have shown that these are not of great importance when considering random systems. In the case of monodisperse samples, for example, their contribution is less than 2% even for filling factors as high as 0.3. The higher the filling factor and the broader the distribution, the more important the higher multipoles become. In any case, for the ranges of f and σ treated here their contribution is much smaller than the effect of polydispersity which is studied below. Thus, we present here calculations that take account of the dipole moment only.

The results are subject to systematic errors originating from the unavoidably limited size of the sample. There are errors due to the high proportion of particles in the vicinity of the electrodes compared to what is normally the case for real material measurements. Furthermore, the homogeneity of the spatial distribution is disturbed by not allowing the spheres to cross the cells boundaries. These errors have nevertheless proved to be of little importance and can be neglected. The main source of inaccuracy is the failure to reproduce the continuous distribution with a limited number of particles. In order to control the effect of the sample size we performed simulations on samples of spheres having a log-normal distribution in volume, as described above, as a function of the total number of particles N. In Fig. 3 the calcu-

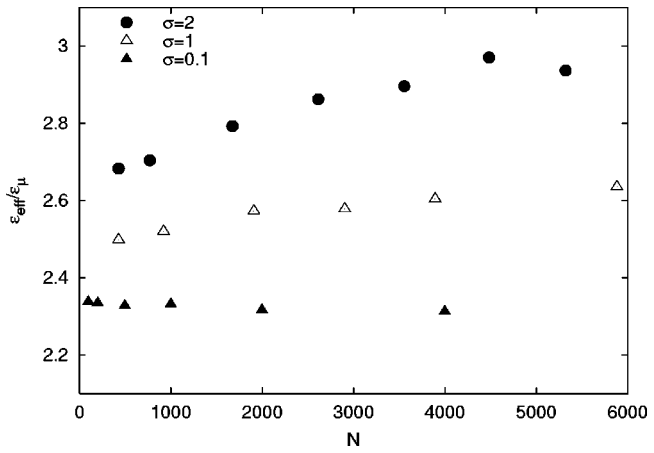

FIG. 3. The convergence of the results with respect to the number of particles. The main factor of the error is the insufficiency of small populations to approximate the continuous distribution.

lated permittivity values are shown for filling factor $f=0.3$ and for $\sigma=2$, $\sigma=1$, and $\sigma=0.1$. For $\sigma=2$, e.g., there is a monotonous change of the calculated ε_{eff} of about 5% between $N=1500$ and $N=3500$, but above $N=3500$ a limiting value seems to be attained, the calculated permittivity fluctuating less than 3%.

Already from Fig. 3 it is obvious that the permittivity values depend on the size distribution width, expressed through the parameter σ. This is shown more clearly in Fig. 4. There the effective dielectric constant is plotted as a function of the filling factor for samples with $\sigma=2$, $\sigma=1$ and for monodisperse systems ($\sigma=0$). For comparison the Maxwell-Garnett and Bruggeman predictions are also plotted. It is evident that the monodisperse systems are accurately described by the Maxwell-Garnett formula (within 2%). The permittivity of polydisperse systems depends not

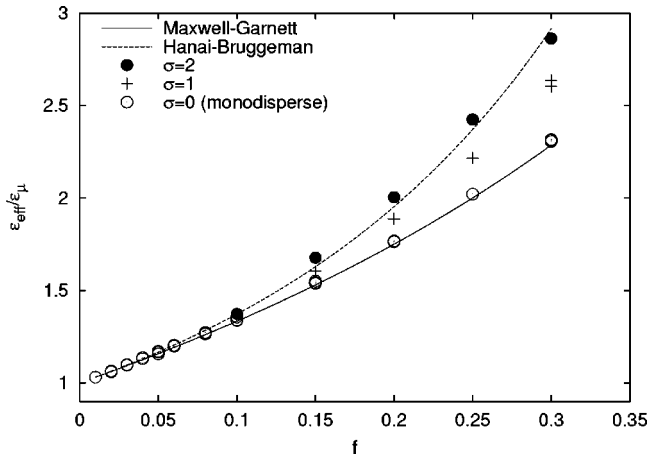

FIG. 4. The ratio $\varepsilon_{\text{eff}}/\varepsilon_\mu$ as a function of the filling factor f for systems with random spatial distribution and log-normal volume distribution with different σ [see Eq. (9)]. The Maxwell-Garnett approximation describes accurately the results for monodisperse systems, while the results for broad distributions (with $\sigma=2$) agree with the Bruggeman formula. The plot makes obvious the dependence of the effective permittivity on the size distribution.

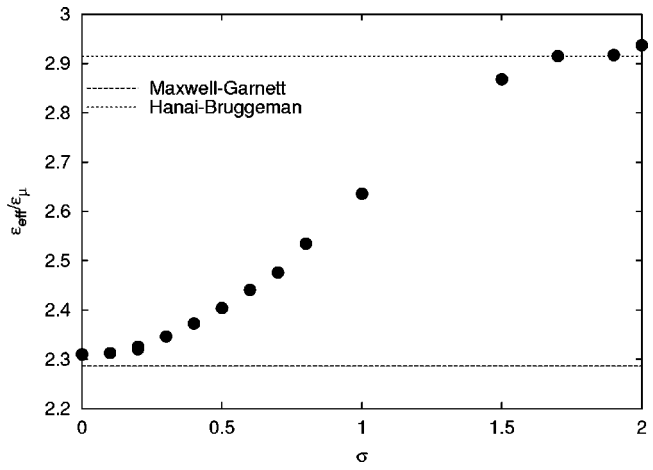

FIG. 5. The ratio $\varepsilon_{\text{eff}}/\varepsilon_\mu$ at $f=0.3$ as a function of the width σ of the log-normal volume distribution [Eq. (9)]. For very narrow and very broad distributions $\varepsilon_{\text{eff}}/\varepsilon_\mu$ tends to values close to those of the Maxwell-Garnett and the Bruggeman models, respectively. The transition occurs in a range around $\sigma=1$.

only on the filling factor, but also on the degree of polydispersity. For $\sigma=2$ it is well described by the Bruggeman formula, while for $\sigma=1$ it lies between this and the Maxwell-Garnett result.

In order to study the transition from one response type to the other, we performed simulations on systems with fixed filling factor ($f=0.3$) varying the width parameter σ of the volume distribution. The results are presented in Fig. 5 as a plot of the effective dielectric constant vs σ. The effective dielectric constant increases monotonously from values very near the Maxwell-Garnett results (for low σ) and approaches a limiting value as σ increases. This value is close to the Bruggeman result. Simulations at higher σ are necessary to determine whether ε_{eff} remains constant. Such simulations require a higher particle population in order to adequately represent the particle volume distribution and can be very time consuming, since the CPU time needed is roughly proportional to N^2.

V. DISCUSSION

It is evident that the permittivity (and correspondingly all generalized conductivities) of matrix-inclusion composite materials shows a sensitive dependency on the size distribution. The Maxwell-Garnett model, which being a dipole approximation has been considered satisfactory for dilute systems only, describes adequately random monodisperse systems even for filling factors as high as 0.3. The Bruggeman model describes well the opposite limit of broad size distributions. In both these mean field formulas the effective permittivity is independent of σ or, generally speaking, the width of the size distribution. So, they can only give a satisfactory description when $d\varepsilon_{\text{eff}}/d\sigma \to 0$, i.e., in the limiting cases of very narrow or very broad distributions (see Fig. 5). It is nevertheless surprising how good the agreement between the complicated calculations and these simple models is, especially keeping in mind that these formulas are derived

without any assumptions whatsoever regarding the size distribution. (Note that Bruggeman only assumes a polydisperse system in order to be able to reach the limit $f \to 1$, that is, to fill the whole space with inclusions. This fact does not explicitly enter his derivation of ε_{eff}.) In most experimental investigations, especially regarding materials for industrial applications and microcomposites or nanocomposites, one deals with large size distributions. Monodisperse systems are seldom encountered in practice and are rather difficult to prepare. Together with Fig. 5 this explains the success of the Bruggeman result in the analysis of experimental data on nonagglomerating systems.

Starting from their exact solution [Eq. (8)] Fu *et al*. have shown analytically that the Maxwell-Garnett formula follows in the mean field approximation, when a spherical symmetric two-particle function is used to describe the spatial distribution of the inclusions.[5] However, Barrera *et al*.[11] have shown that in the case of polydisperse systems the correlated fluctuations of the induced dipole moments play a vital role and cannot be neglected. They lead to higher interparticle interactions and thus to an increased permittivity. An iterative procedure, such as the one followed by Bruggeman, might take care of some of these effects.[18]

The dependence on the particle size distribution can be intuitively understood as follows: The interaction between the dipolar moments of the particles i,j is proportional to the quantity $1/r_{ij}^3$, the inverse cube of their distance (see the Appendix). The interparticle distances decrease (and thus the capacitances between them increase) with the polydispersity. Concluding, a formula which would describe the effective permittivities of polydisperse systems, especially in the transition range (around $\sigma = 1$), has to contain explicitly the particle size distribution.

ACKNOWLEDGMENTS

This work was supported by the European Commission under TMR Marie Curie Grant No. ERBFMBICT982913 (A.S.) and by the DFG under Project No. Ni/49/33-1. We are grateful to the Institut für Elektrotechnik, Universität Magdeburg and especially to Dr. H. G. Krauthäuser, for the CPU time that was made available to us.

APPENDIX

For the sake of completeness and convenience of the reader, we give here the form of the configuration matrix G. We do not comment in detail, since this form is only slightly different from the one given in Ref. 5. The only difference is that periodic boundary conditions in the plane parallel to the capacitor's electrodes are introduced. The central idea is that the interaction with the periodic repetitions of the particles can be integrated in the interaction with their equivalent particle in the main shell, just as it happens with the image particles in the treatment of Fu, Macedo, and Resca. Choosing the index k to count the images and ξ to count the periodic repetitions

$$G_{ilm}^{jl'm'} = \delta_i^j \delta_l^{l'} \delta_m^{m'} + (2l+1)\beta_{il} C_{lm}^{l'm'}(\mathbf{r}_j - \mathbf{r}_i), \tag{A1}$$

where

$$C_{lm}^{l'm'}(\mathbf{r}_j - \mathbf{r}_i) = \sum_{\xi k} (-1)^{(l'+m'+1)k} A_{lm}^{l'm'} \times (\mathbf{r}_{j\xi k} - \mathbf{r}_i)(1 - \delta_i^j \delta_\xi^0 \delta_k^0), \tag{A2}$$

$$\beta_{il} = \frac{(\varepsilon_i - \varepsilon_\mu) l \alpha_i^{2l+1}}{l\varepsilon_i + (l+1)\varepsilon_\mu}, \tag{A3}$$

and

$$A_{lm}^{l'm'}(\mathbf{r}_{j\xi k} - \mathbf{r}_i) = \frac{Y^*_{l+l',m-m'}(\mathbf{r}_{j\xi k} - \mathbf{r}_i)}{|\mathbf{r}_{j\xi k} - \mathbf{r}_i|^{l+l'+1}} (-1)^{l'+m'} \times \left[\frac{4\pi (l+l'+m-m')!(l+l'-m+m')!}{(2l+1)(2l'+1)(2l+2l'+1)(l+m)!(l-m)!(l'+m')!(l'-m')!} \right]^{1/2}. \tag{A4}$$

In the above relations $\mathbf{r}_{i\xi k}$ is the position vector of the ξth periodic repetition of the kth image of the particle i. Apart from the additional index ξ these are the expressions presented in Ref. 5.

Taking into account dipole moments only, for a sample with infinite dimensions (so that images and periodic repetitions need not be considered) this reduces to

$$G_{ilm}^{jl'm'} = \delta_i^j - (1-\delta_i^j)\frac{\alpha_i^3}{r_{ij}^3}(3\cos^2\theta - 1). \qquad \text{(A5)}$$

Thus, in this approximation, the term $(G^{-1})_{ilm}^{j10}\beta_{j1}E_0$ inside the sum in Eq. (6), is approximately proportional to $1/r_{ij}^3$.

In our implementation, suitable parameters determine the number $k_{\max}$ of image particles and $\xi_{\max}$ of periodical repetitions that are considered, according to the desired numerical accuracy. These numbers are not the same for every particle pair, but depend on the strength of the interaction. Typically, a few thousand images enter the calculation as well as periodic repetitions at distances up to 5–7 times the sample dimensions.

*Electronic address: anna@obelix.ph2.uni-koeln.de

[1] J. W. S. Rayleigh, Philos. Mag. **34**, 481 (1892).
[2] J. C. Maxwell, *A Treatise on Electricity and Magnetism*, 3rd ed. (Dover Publications, New York, 1954), Vol. 2.
[3] R. Pelster, Phys. Rev. B **59**, 9214 (1999).
[4] R. Pelster and U. Simon, Colloid Polym. Sci. **277**, 2 (1999).
[5] L. Fu, P. M. Macedo, and L. Resca, Phys. Rev. B **47**, 13 818 (1993).
[6] J. C. M. Garnett, Philos. Trans. R. Soc. London **203**, 385 (1904).
[7] S. S. Dukhin, in *Surface Colloid Science*, edited by E. Matijevic (Interscience, New York, 1967), Vol. 3, Chap. Dielectric Properties of disperse systems, pp. 83–165.
[8] L. K. H. van Beek, in *Progress in Dielectrics* (Heywood, London, 1967), Vol. 7, Chap. 3, pp. 69–114.
[9] D. A. G. Bruggeman, Ann. Phys. (N.Y.) **24**, 636 (1935).
[10] This result for polydisperse systems follows readily from Eq. (B11) in Ref. 5 taking α^s constant and $\Sigma v^s = f$.
[11] R. G. Barrera, P. Villaseñor-González, W. L. Mochán, and G. Monsivais, Phys. Rev. B **41**, 7370 (1990).
[12] R. E. Meredith and C. W. Tobias, J. Electrochem. Soc. **108**, 286 (1961).
[13] K. Günther and D. Heinrich, Z. Phys. **185**, 345 (1965).
[14] D. R. McKenzie, R. C. McPhedran, and G. H. Derrick, Proc. R. Soc. London, Ser. A **362**, 211 (1978).
[15] R. E. Meredith and C. W. Tobias, J. Appl. Phys. **31**, 1270 (1960).
[16] R. C. McPhedran and D. R. McKenzie, Proc. R. Soc. London, Ser. A **359**, 45 (1978).
[17] W. H. Press, S. A. Teukolsky, W. T. Vetterling, and B. P. Flannery, *Numerical Recipes in C, The Art of Scientific Computing*, 2nd ed. (Cambridge Univerity Press, Cambridge, 1992).
[18] R. Fuchs and K. Ghosh, Physica A **207**, 185 (1994).